

Understanding the dynamical status of Galactic Globular Cluster NGC 6656

Gaurav Singh^{1,2}  and R. K. S. Yadav¹

¹Arybhata Research Institute of Observational Sciences, Manora Peak, Nainital 263002, India
emails: gaurav@aries.res.in, rkant@aries.res.in

²Dept. of Physics & Astrophysics, University of Delhi, Delhi 110007, India

Abstract. We present the study of horizontal branch morphology of the cluster NGC 6656. A blueward shift in temperature of about ~ 5000 K (nM-jump) in the color-color plot is detected. To explain this feature, we study the presence of stellar-mass black hole by plotting Projected density profile (PDP) in the central HST region. The PDP in the inner region ($r < 10''$) can be nicely reproduced by the king+BH model. The blue ward shift in temperature can be due the presence of stellar mass black holes in the centre.

Keywords. (stars:) blue stragglers; stars: black holes; stars: horizontal branch

1. Introduction

Globular clusters (GCs) are spherical agglomeration of stars and are centrally dense systems. These stellar systems are among the oldest stellar systems orbiting their host galaxies. Because of high stellar densities of these systems, several dynamical processes occur, like stellar collisions, core collapse, stellar mergers and two-body relaxation (Meylan & Heggie (1997)). These dynamical interactions lead to several exotic populations, such as blue straggler stars (BSSs), low mass millisecond pulsars and cataclysmic variables, etc. Blue stragglers constitutes the largest population among all these exotic population therefore are very important candidates for dynamical studies of GCs. Based on the shape of observed BSS radial distribution, Ferraro *et al.* (2012) grouped BSS into three families corresponding to different dynamical ages. We studied the BSS radial distribution of the GGC NGC 6656 and found it to be an intermediate dynamical status (Singh & Yadav (2019)). However, it has been found that, the process of BSS segregation can be delayed by the presence of dark remnants, in particular, by a significant population of stellar mass black holes (Lanzoni *et al.* 2016). Strader *et al.* (2012) discovered two stellar mass black holes that are accreting matter in the central region of the cluster NGC 6656.

GCs also harbor other stellar population which are a result of dynamical interactions of the system, like early and late helium flashers, which governs the tail of Horizontal Branch (HB) morphology. In the clusters having sufficiently broad distribution of HB in color, various discontinuities are seen. These discontinuities appear in form of gaps, jumps and sub-luminous stars depending upon the band-passes employed. The most common among these discontinuities are “Grundahl jump” (G-jump) and “Momyan jump” (M-jump) which appear at $\sim 11,500$ K and $\sim 20,000$ K respectively. The presence of black holes in the cluster can influence the tail of HB morphology. (Miocchi (2007)) found the presence of intermediate-mass black holes in globular clusters and their connection with extreme horizontal branch stars.

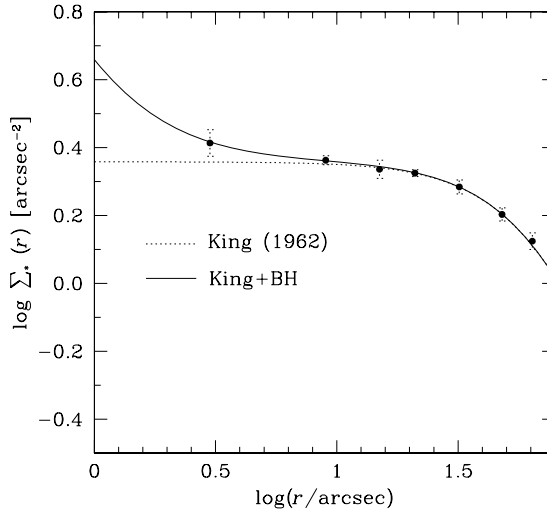


Figure 1. The observed Projected density profile of NGC 6656 is plotted. The profile in the inner region is nicely reproduced by King+BH model, whereas in the outer region the profile follows the king (1962) model.

2. Data used

We used the astro-photometric catalogue (Nardiello *et al.* 2018) for the present study. The catalogue contains the photometric data in $F275W$, $F336W$ and $F438W$ filters, which are taken through HST WFC3/UVIS channel. The catalogue also contains the proper motion membership information of all the stars. We used only the stars with the membership probability $\geq 90\%$.

3. Results & Discussions

3.1. Projected density profile

To see the effect of stellar mass black holes, we constructed the Projected density profile (PDP) in the central region, starting from C_{grav} to $\sim 90''$. For the completeness of the sample we used only $F606W$ brighter than 21 mag. We used the value of C_{grav} and structural parameters obtained from Singh & Yadav (2019) and fitted the king profile in the outer region ($10'' < r < 90''$). The PDP shown in Fig. 1 exhibits a density cusp in the inner region ($r < 10''$).

The observed features in the PDP derived in the inner region can be due to the presence of stellar-mass black holes in central region of the cluster NGC 6656. Stars are expected to form a density cusp in the power-law form $\rho(r) \propto r^{-7/4}$ near the black hole (Miocchi (2007)). The theoretical representation of stellar density due to the BH presence near the cluster centre is given by, $\rho(r) \simeq \rho_{unperturbed}(r)[1 + (r_h/r)^{7/4}]$ (Bahcall & Wolf (1976)), where r_h is defined as the BH radius of influence. In order to reproduce this feature, we first need to estimate r_h , which is given by $r_h = GM_{BH}/\sigma_o^2$, where M_{BH} is the BH mass and σ_o is the velocity dispersion outside r_h . By considering $\sigma_o = 6.65 \text{ km s}^{-1}$ (Peterson & Cudworth (1994)) and $M_{BH} = 15 M_\odot$ (Strader *et al.* 2012), we estimated $r_h \simeq 0.015 \text{ pc}$, corresponding to $\sim 1''$ at a cluster distance of 3.2 kpc. The profile is well reproduced by King+BH model in the inner region as shown in Fig. 1.

3.2. Horizontal branch morphology

Our main aim is to study the color-color plot (color index $C_{F275W,F336W,F438W} = (m_{F275W} - m_{F336W}) - (m_{F336W} - m_{F438W})$ versus intrinsic $(m_{F275W} - m_{F438W})$ color.

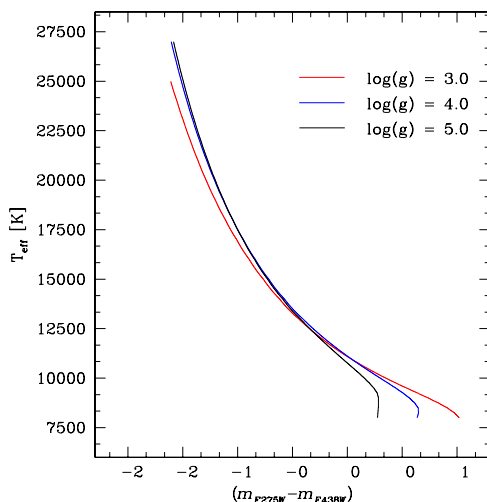


Figure 2. The color-temperature relationship of the HB stars for different $\log(g)$ values.

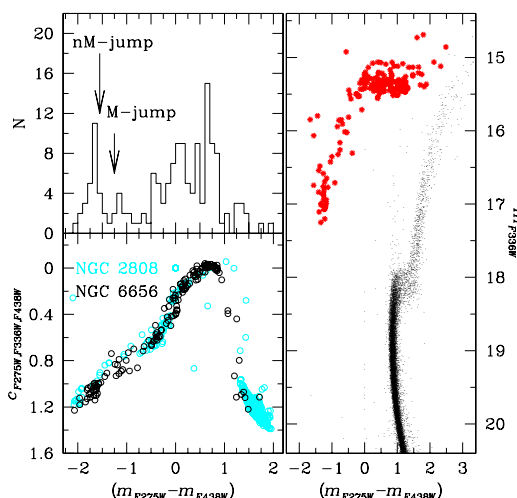


Figure 3. The color-color plot along with histogram is plotted in the left panels. The HB stars of NGC 6656, used for color-color plot is shown as red points in right panel.

To study this, we obtained the color-temperature relationship for HB morphology of the cluster NGC 6656. For this purpose, we convolved the atmospheric models with the WFC3/UVIS filter effective area curves.

We selected model spectra within $8,000 \text{ K} \leq T_{eff} \leq 27,000 \text{ K}$ and $3.0 \leq \log(g) \leq 5.0$ to derive the dereddened color-temperature relationship for stars lying between C_{peak} and near M-jump in color-color plot. NGC 2808 is taken as a reference cluster of the color-color plot study. In Fig. 2, the color-temperature relationship for the reference cluster NGC 2808, with $[\text{Fe}/\text{H}] = -1.36$ and for the $\log(g)$ of 3.0, 4.0 and 5.0 are plotted.

In Fig. 3, the color-color plot of HB stars of NGC 6656 is over plotted on the color-color plot of NGC 2808 with a shift of $(-3.30, -0.04)$ mag. By considering the metallicity value of $[\text{Fe}/\text{H}] = -1.36$ for NGC 2808, we obtained the effective temperatures of the C_{peak} ($\sim 8600 \text{ K}$), the G-jump ($\sim 11,500 \text{ K}$), and the M-jump ($\sim 20,000 \text{ K}$) respectively. The

color-color plot of NGC 6656 however, show a blue ward shift in the M-jump, with a temperature shift of about ~ 5000 K (nM-jump).

Since, M-jump occur as an onset of extreme horizontal branch stars, this feature can be due to the presence of stellar-mass black holes that are accreting in the central region. There could be other possible explanation of such blueward shift, i.e., since the M-jump is sensitive to the metallicity changes, that increasing $[\text{Fe}/\text{H}]$ extend the He II convection zone to both hotter temperatures and shallower depths (Brown *et al.* 2016). The metallicity spread in the cluster NGC 6656 is $-1.4 \leq [\text{Fe}/\text{H}] \leq -1.9$ (Lee (2015)), which can lead to a temperature shift of about ~ 5000 K. However, a complete understanding of which one is dominant can be revealed by further theoretical and spectroscopic studies.

Acknowledgment

We used pysynphot synthetic photometry software package for obtaining the color-temperature relationship of HB stars.

References

- Bahcall, J. N. & Wolf, R. A. 1976, *ApJ*, 209, 214
- Brown, T. M., Cassisi, S., Antona, F. D., Salaris, M., Milone, A. P., Dalessandro, E., Piotto, G., Renzini, A., Sweigart, A. V., Bellini, A., Ortolani, S., Sarajedini, A., Aparicio, A., Bedin, L. R., Anderson, J., Pietrinferni, A., & Nardiello, D. 2016, *ApJ*, 822, 44
- Ferraro, F. R., Lanzoni, B., Dalessandro, E., Beccari, G., Pasquato M., Miocchi P., Rood, R. T., Sigurdsson, S., Sills, A., Vesperini, E., Mapelli, M., Contreras, R., Sanna, N., & Mucciarelli, A. 2012, *Nature*, 492, 393
- Lanzoni, B., Ferraro, F. R., Alessandrini, E., Dalessandro, E., Vesperini, E. & Raso, S. 2016, *ApJL*, 833, 129
- Lee, J. W. 2015, *ApJS*, 219, 7
- lim, P. L., Diaz, R. I., & Laidler, V. 2015, *PySynphot User's Guide* (Baltimore, MD: STScI)
- Meylan, G. & Heggie, D. C. 1997, *A&A Rev.*, 8, 1
- Miocchi, P. 2007, *MNRAS*, 318, 103
- Nardiello, D., Libralato, M., Piotto, G., Anderson, J., Bellini, A., Aparicio, A., Bedin, L. R., Cassisi, S., Granata, V., King, I. R., Lucertini, F., Marino, A. F., Milone, A. P., Ortolani, S., Platais, I. & van der Marel, R. P. 2018, *MNRAS*, 481, 3382
- Peterson, R. C., & Cudworth, K. M. 1994, *ApJ*, 420, 612
- Singh, G. & Yadav R. K. S. 2019, *MNRAS*, 482, 4874
- Strader, J., Chomiuk, L., Maccarone, T. J., Miller-Jones, J. C. A., & seth, A. C. 2012, *Nature*, 490, 71